

NUMERICAL MODELLING OF TWO-PHASE FLOW A BENCHMARK SOLUTION

Darrin W. STEPHENS and Jonathan A. HARRIS

School of Engineering, Mechanical Engineering
 James Cook University, Townsville, Queensland, AUSTRALIA

ABSTRACT

This paper explores a simple test problem that can be used as a benchmark solution for Eulerian two-phase flow CFD models. Results are presented for a commercial CFD code with multiphase flow capability, namely CFX-4.2, produced by AEA Technology. The results show that CFX-4.2 exhibits virtually perfect agreement for all 17 test cases covering a wide range of input parameters.

INTRODUCTION

In order to gain confidence in the accuracy of commercial two-phase flow CFD codes it is often necessary to study simple two-phase flow problems with known solutions. In this way issues such as mesh requirements, choice of solver parameters and implementation of user-defined subroutines may be investigated thoroughly before the code is applied to more complex problems in which the solution is unknown. This step is particularly important in multiphase flow as the solutions can often be complex and non-intuitive.

GOVERNING EQUATIONS

The equations governing Eulerian multiphase fluid-fluid flows are presented in chapter 12 of the CFX-4.2 Solver manual (Anon., 1997). Each phase, denoted by α , interpenetrates with the other phases and occupies a volume fraction r_α . For N_p phases, the sum of the volume fractions must equal unity, viz:

$$\sum_{\alpha=1}^{N_p} r_\alpha = 1 \quad (1)$$

The continuity equation for phase α is

$$\frac{\partial}{\partial t}(r_\alpha \rho_\alpha) + \nabla \cdot (r_\alpha \rho_\alpha \vec{u}_\alpha) = \sum_{\beta=1}^{N_p} (\dot{m}_{\alpha\beta} - \dot{m}_{\beta\alpha}) \quad (2)$$

where \vec{u}_α is the velocity of phase α , ρ_α is the density of phase α and $\dot{m}_{\alpha\beta}$ characterises the mass

transfer from phase β to phase α . Note that $\dot{m}_{\alpha\alpha} = 0$. Assuming no body forces or momentum sources the conservation of momentum equation for phase α is

$$\begin{aligned} \frac{\partial}{\partial t}(r_\alpha \rho_\alpha \vec{u}_\alpha) + r_\alpha \nabla p_\alpha + \nabla \cdot (r_\alpha (\rho_\alpha \vec{u}_\alpha \otimes \vec{u}_\alpha)) \\ - \nabla \cdot (\mu_\alpha (\nabla \vec{u}_\alpha + (\nabla \vec{u}_\alpha)^T)) = \\ \sum_{\beta=1}^{N_p} c_{\alpha\beta}^{(d)} (\vec{u}_\beta - \vec{u}_\alpha) + \sum_{\beta=1}^{N_p} (\dot{m}_{\alpha\beta} \vec{u}_\beta - \dot{m}_{\beta\alpha} \vec{u}_\alpha) \quad (3) \end{aligned}$$

where $c_{\alpha\beta}^{(d)}$ is the interphase drag coefficient. The interphase mass transfer is defined as follows:

$$\dot{m}_{\alpha\beta} = \max(-s_{\alpha\beta}, 0), \quad \dot{m}_{\beta\alpha} = \max(s_{\alpha\beta}, 0)$$

where $s_{\alpha\beta}$ is the mass flow rate per unit volume from phase α to phase β .

Thus :

$$\begin{aligned} s_{\alpha\beta} \geq 0 &\Rightarrow \dot{m}_{\alpha\beta} = 0, \quad \dot{m}_{\beta\alpha} = s_{\alpha\beta} \\ s_{\alpha\beta} \leq 0 &\Rightarrow \dot{m}_{\alpha\beta} = -s_{\alpha\beta}, \quad \dot{m}_{\beta\alpha} = 0 \end{aligned}$$

The above equations apply to the general case of N_p phases. In what follows, a simplified set of these equations will be derived that apply to one-dimensional two phase flow with mass and/or momentum transfer. This case has a known solution and so is ideal for development and validation of two-phase flow numerical solutions. For example, when developing mass and momentum transfer subroutines it is best to solve a problem with a known solution to ensure that the subroutines have been implemented correctly.

One-dimensional two-phase flow

Consider the case of steady state, incompressible flow in a horizontal channel of constant cross section. It is assumed that one-dimensional flow occurs so that all quantities have uniform (i.e., constant) profiles at any x position and that all phases experience the same pressure. Also, assume that only two phases are present (f and g),

and that there is a mass transfer rate per unit volume of \dot{m} from phase f to phase g (i.e., $s_{fg} = \dot{m}$). Further, let the volume fraction of phase f be r_f so that, by continuity, the volume fraction of phase g is $1 - r_f$. Under these assumptions the continuity equations simplify to

$$\frac{d}{dx}[(1 - r_f)\rho_g u_g] = \dot{m} \quad (4)$$

$$\frac{d}{dx}(r_f \rho_f u_f) = -\dot{m} \quad (5)$$

and the momentum equations to

$$-(1 - r_f)\frac{dp}{dx} + u_f \dot{m} + c_{fg}^{(d)}(u_f - u_g) = \frac{d}{dx}[(1 - r_f)\rho_g u_g^2] \quad (6)$$

$$-r_f \frac{dp}{dx} - u_f \dot{m} + c_{fg}^{(d)}(u_g - u_f) = \frac{d}{dx}(r_f \rho_f u_f^2) \quad (7)$$

In the above momentum equations the shear stress terms, such as $d(r_f \mu_f du_f/dx)/dx$, have been omitted since they can be made negligibly small by choosing a low viscosity. These equations may be rearranged to yield the following set of coupled ordinary differential equations in the four unknowns r_f , u_g , p and u_f :

$$\frac{dr_f}{dx} = \frac{\left[\frac{\dot{m} r_f}{\rho_f (1 - r_f)} - \frac{\dot{m}}{\rho_f} - \frac{2\dot{m} r_f u_g}{u_f \rho_f (1 - r_f)} - \frac{c_{fg}^{(d)}(u_g - u_f)}{u_f^2} \right]}{u_f \left[1 + \frac{r_f \rho_g u_g^2}{\rho_f u_f^2 (1 - r_f)} \right]} \quad (8)$$

$$\frac{du_g}{dx} = \frac{\left[\dot{m} + u_g \rho_g \frac{dr_f}{dx} \right]}{(1 - r_f)\rho_g} \quad (9)$$

$$\frac{dp}{dx} = \left[\frac{\dot{m}}{(1 - r_f)} + c_{fg}^{(d)} \rho_f \right] (u_f - u_g) - \rho_g u_g \frac{du_g}{dx} \quad (10)$$

$$\frac{du_f}{dx} = \frac{(1 - r_f)c_{fg}^{(d)}(u_g - u_f)}{\rho_f u_f r_f} - \frac{1}{u_f \rho_f} \frac{dp}{dx} \quad (11)$$

If the conditions at the channel inlet are known, these equations may be integrated along the channel (e.g., using the ODE solver routines in MatlabTM) to yield profiles of r_f , u_g , p and u_f . The mass transfer per unit volume from phase f to phase g (\dot{m}) must either be given (e.g., a constant) or expressed in terms of the solution variables. In this study the following equation was used to compute \dot{m} , since this is used by CFX:

$$\dot{m} = C_M r_g \rho_f \quad (12)$$

Here C_M is a constant with units of inverse seconds. The interphase drag coefficient $c_{fg}^{(d)}$ is defined by

$$c_{fg}^{(d)} = \frac{3C_d}{4d} |u_g - u_f| \quad (13)$$

where d is the particle diameter and C_d is the drag coefficient. The drag coefficient can be given (e.g., a constant) or expressed in terms of the solution variables. In this study the drag coefficient will be given a constant value.

NUMERICAL MODELLING

In this section a commercial code with multiphase flow capabilities is applied to solve the test problem identified above. The code is CFX-4.2, produced by AEA Technology. The one-dimensional

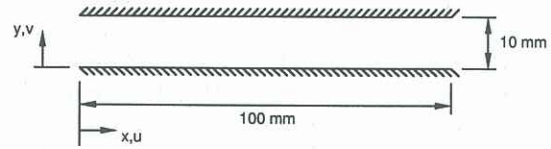


Figure 1: Channel geometry used for simulations

flow test problem was solved using the geometry shown in Figure 1. The parallel plates are 100 mm long with a plate separation of 10 mm. Properties and further solution details are given in the following sections.

One-dimensional two-phase flow without drag MATLABTM.

Equations (8) through (12) were solved numerically using the fourth and fifth order Runge-Kutta algorithm (ode45) implemented in MATLABTM. The drag coefficient C_d in equation (13) was set to zero. The mass transfer rate \dot{m} was computed from equation (12) using the values of C_M given in Table 1. The relative error solution tolerance was set to 10^{-8} . The problem requires that the values of u_f , u_g and r_f are specified at the channel inlet ($x = 0$). In addition, the fluid densities (ρ_f and ρ_g) must also be specified. A total of 12 different cases were run, covering a range of fluid densities, inlet velocities and inlet volume fractions, as shown in Table 1. Table 2 summarises the results of these different runs. The values given in the last three columns of Table 2 correspond to the values of u_f , u_g and r_f , respectively, at the outlet of the one-dimensional channel. Figure 2 shows a plot of the primary phase velocity (u_f), secondary phase velocity (u_g), primary phase volume fraction (r_f) and pressure versus streamwise position along the channel for case 12. For this particular case there is not a large change in some of the solution variables (e.g., u_f changes from an inlet

Run	C_M (s^{-1})	ρ_f (kg/m^3)	ρ_g (kg/m^3)	u_f (m/s)	u_g (m/s)	r_f (-)
1	3	1	1	2	2	0.8
2	3	1	1	1	2	0.8
3	3	1	1	4	2	0.8
4	3	1	1	2	1	0.8
5	3	1	1	2	4	0.8
6	3	1	1	2	2	0.5
7	3	1	1	2	1	0.5
8	3	2	1	2	2	0.5
9	0.1	50	1	2	2	0.5
10	0.1	1000	1	2	2	0.8
11	3	1	2	1	2	0.8
12	0.01	997	0.0256	2	0.01	0.8

Table 1: Parameters and inlet conditions for model runs without drag.

value of 2 to an outlet value of 2.0179, whereas r_f changes from 0.8 at the inlet to 0.7928 at the outlet). Some of the other cases (e.g., case 9) show substantial variation in the velocities and volume fractions along the channel.

CFX-4.2.

One-dimensional two-phase flow can be implemented on a two-dimensional geometry by applying a boundary condition of zero shear stress at the channel walls. A uniform mesh of 40 cells in the x direction and 10 cells in the y direction was used in all cases without drag. The applied inlet conditions are uniform across the channel and correspond to the values given in Table 1. Convergence testing was applied to the continuity equation with a convergence value of 1×10^{-7} kg/s. No initial guess was patched to the computational domain. Figure 2 shows a plot of the primary phase velocity (u_f), secondary phase velocity (u_g), primary phase volume fraction (r_f) and pressure versus streamwise position along the channel for case 12. Due to the large density ratio, case 12 was the most difficult to solve requiring large under relaxation of the mass transfer term for the solution to converge.

Comparison with MATLABTM solution.

Assuming that the numerical MATLABTM solutions given in Table 2 are at least accurate to the number of significant figures shown, then a comparison between the results given by CFX-4.2 to those given by MATLABTM can be made. The results from CFX-4.2, shown in Figure 2, show near perfect agreement with the MATLABTM predictions. Additionally, the solution values at the channel outlet (given in Table 2) also show near perfect agreement with the MATLABTM predictions, over the full range of test cases. At worst, there are differences in the second decimal place of the solution, which is considered excellent for the relatively coarse mesh used. Figure 2

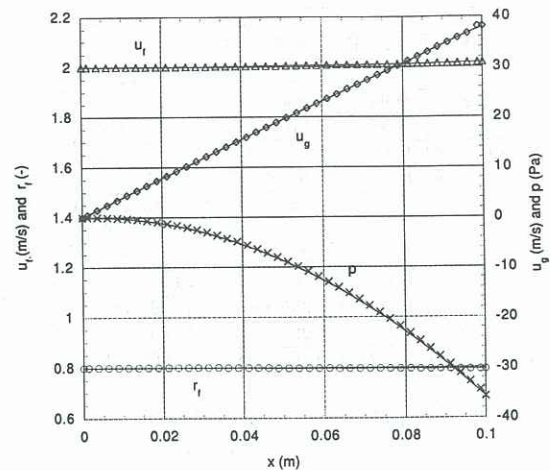


Figure 2: Comparison of MATLABTM and CFX-4.2 results for run 12. Inlet conditions and parameters are given in Table 1. Solid lines and symbols correspond to MATLABTM computations and CFX-4.2 results, respectively.

shows that as mass is transferred from phase f to phase g the velocity of phase f increases slightly, while the velocity of phase g increases drastically. The continuity equations (4) and (5) for phase g and phase f respectively, allow for the explanation of the results shown. Since the density of phase g is small compared to phase f , phase g must accelerate to satisfy continuity. From the conservation of momentum, equations (6) and (7), this acceleration of phase g causes a decrease in the pressure along the length of the channel as shown in Figure 2.

One-dimensional two-phase flow with drag MATLABTM.

The solution of the problem with mass and momentum exchange requires the drag coefficient and particle diameter in equation (13) to be set, values of 0.5 and 1.0mm were used. A total of 5 different cases were run, covering a range of inlet velocities and inlet volume fractions, as shown in Table 3. Table 4 summarises the results of these different runs. Figure 3 shows a plot of the primary phase velocity (u_f), secondary phase velocity (u_g), primary phase volume fraction (r_f) and pressure versus streamwise position along the channel for case 5.

CFX-4.2.

The applied inlet conditions and model parameters correspond to case 5 given in Table 3. Figure 3 shows a plot of the primary phase velocity (u_f), secondary phase velocity (u_g), primary phase volume fraction (r_f) and pressure versus streamwise position along the channel for case 5.

Run	u_f (m/s)		u_g (m/s)		r_f (-)	
	CFX	M'LAB	CFX	M'LAB	CFX	M'LAB
1	2	2	2	2	0.7676	0.7676
2	0.981	0.981	1.8385	1.8449	0.7455	0.7465
3	3.968	3.968	2.2070	2.2071	0.7910	0.7910
4	1.9722	1.9722	1.1915	1.1915	0.7794	0.7794
5	1.9817	1.9817	3.8429	3.8431	0.7753	0.7753
6	2	2	2	2	0.4190	0.4191
7	1.9515	1.9514	1.1588	1.1588	0.4305	0.4305
8	2.1098	2.1100	2.2017	2.2017	0.3955	0.3955
9	3.3232	3.3294	13.8019	13.8019	0.2440	0.2437
10	2.0533	2.0533	11.2061	11.1993	0.7782	0.7782
11	1.965	1.965	1.9819	1.9819	0.7824	0.7824
12	2.0179	2.0178	38.0751	38.0591	0.7928	0.7928

Table 2: Comparison of MATLABTM and CFX-4.2 results at the channel outlet for cases without drag.

Run	C_M (s^{-1})	ρ_f (kg/m^3)	ρ_g (kg/m^3)	u_f (m/s)	u_g (m/s)	r_f (-)
1	0.001	997	0.0256	1	2	0.8
2	0.001	997	0.0256	2	1	0.8
3	0.001	997	0.0256	1	1	0.5
4	0.001	997	0.0256	0.1	1	0.5
5	0.001	997	0.0256	1	0.1	0.5

Table 3: Parameters and inlet conditions for model runs with drag.

A uniform mesh of 500 cells in the x direction and 10 cells in the y direction was used in all cases with drag.

Comparison with MATLABTM solution.

The results from CFX-4.2, shown in Figure 3, show near perfect agreement with the MATLABTM predictions. Additionally, the solution values at the channel outlet (given in Table 4) also show near perfect agreement with the MATLABTM predictions, over the full range of test cases. Mesh refinement of the CFX models was required to achieve the accuracy of the results shown in Table 4. Using the mesh used for the solutions without drag gave agreement to the first decimal place with the MATLABTM solutions. The number of steps MATLABTM took to solve the problem was used to indicate the mesh refinement needed in the CFX models. The number of elements required by CFX can be reduced if mesh biasing is used instead of the uniform mesh but this was not investigated in the study. Figure 3 shows that at the entrance of the channel a rapid adjustment in the flow velocities takes place. This is attributed to the drag between the phases. As mass is transferred from phase *f* to phase *g* the velocity of phase *f* increases, as does the velocity of phase *g*. The increase in phase velocity of

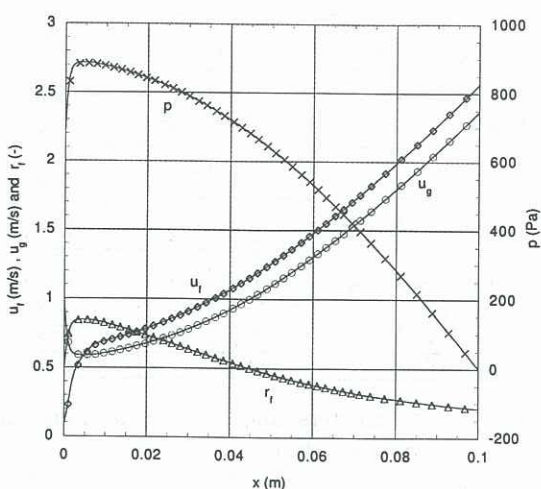


Figure 3: Comparison of MATLABTM and CFX-4.2 results for run 5. Inlet conditions and parameters are given in Table 3. Solid lines and symbols correspond to MATLABTM computations and CFX-4.2 results, respectively.

Run	u_f (m/s)		u_g (m/s)		r_f (-)	
	CFX	M'LAB	CFX	M'LAB	CFX	M'LAB
1	3.2282	3.2279	3.4782	3.4742	0.2478	0.2478
2	2.6388	2.6390	2.8879	2.8870	0.6063	0.6063
3	3.6641	3.6651	3.8755	3.8781	0.1364	0.1364
4	4.2563	4.2585	4.3300	4.3309	0.0117	0.0117
5	2.3647	2.3685	2.5681	2.5678	0.2111	0.2114

Table 4: Comparison of MATLABTM and CFX-4.2 results at the channel outlet.

phase *g* is not as drastic as was for the cases without drag. This shows that the addition of drag to the one-dimensional two-phase flow problem has the effect of reducing the difference between the phase velocities, as expected.

CONCLUSIONS

A simplified two-phase flow problem has been given that can be used for benchmarking of multiphase flow CFD codes. The case of one-dimensional two-phase flow with mass and momentum transfer results in a system of coupled ODEs which can be integrated with high accuracy. The performance of a commercial CFD code, CFX-4.2, was evaluated by applying it to solve the test problem. The results show that CFX-4.2 exhibits virtually perfect agreement with test cases over a range of input parameters.

REFERENCES

ANON., *CFX-4.2 Solver Manual*, CFX International, Harwell, Didcot, Oxfordshire, 1997.